

HIGGS BOSON DECAY INTO GLUONS: IR CANCELLATION IN THE DECAY RATE AT NLO USING IMPLICIT REGULARIZATION*

ANA ISABEL PEREIRA, BRIGITTE HILLER

CFisUC, Department of Physics, University of Coimbra
3004-516 Coimbra, Portugal

ADRIANO CHERCHIGLIA

Instituto de Física Gleb Wataghin — Universidade Estadual de Campinas
Campinas-SP, Brasil

MARCOS SAMPAIO

Universidade Federal do ABC, 09210-580, Santo André, Brasil

*Received 11 February 2023, accepted 23 August 2023,
published online 27 October 2023*

The Higgs decay $H \rightarrow gg(g)$ using an effective Higgs–Yang–Mills interaction as well as usual QCD interactions is revisited in the context of Implicit Regularization (IReg) and compared with conventional dimensional regularization (CDR), four dimensional helicity (FDH), and dimensional reduction (DRED) schemes, showing that no evanescent fields such as ϵ -scalars need to be introduced. Unambiguous identification and separation of UV from IR divergences is achieved and UV singularities are removed as usual by renormalization. The IR divergences are cancelled due to the method's compliance with the Kinoshita–Lee–Nauenberg (KLN) theorem.

DOI:10.5506/APhysPolBSupp.16.8-A13

1. Introduction

Regularization frameworks that operate partially or entirely in the physical dimension can bring simplifications in the evaluation of Feynman amplitudes, whereupon extensions such as DRED, FDH, and IReg, among others [1] have been constructed as an alternative to conventional dimensional regularization (CDR).

* Presented at *Excited QCD 2022*, Sicily, Italy, 23–29 October, 2022.

The main goal of this work is the computation of the total decay rate of the $H \rightarrow gg$ decay described by an effective model to NLO. Our objective is twofold: (a) the renormalization of an effective non-Abelian field theory with IReg; (b) the implementation of the KLN theorem [2] with a clear separation of IR/UV scales.

2. UV/IR identification and UV renormalization in IReg

IReg is a regularization method that operates on the momentum space and was shown to respect unitarity, locality, and Lorentz invariance [3]. The main idea of IReg is to use an algebraic identity at the integrand level

$$\frac{1}{(k-p)^2 - \mu^2} = \frac{1}{k^2 - \mu^2} + \frac{2k \cdot p - p^2}{(k^2 - \mu^2)((k-p)^2 - \mu^2)} \quad (1)$$

recursively, until the UV divergent behavior is cast in irreducible loop integrals that depend only on the internal momentum k denoted Basic Divergent Integrals (BDIs). Here, μ is an IR regulator introduced in the massless propagators in conformity with a normal form, which amounts to basic operations such as shift invariance and numerator–denominator consistency being respected in the process of regularization [4]. BDIs can take either logarithmic or quadratic forms which are, respectively,

$$I_{\log}(\mu^2) = \int_k \frac{1}{(k^2 - \mu^2)^2}, \quad \text{and} \quad I_{\text{quad}}(\mu^2) = \int_k \frac{1}{(k^2 - \mu^2)}. \quad (2)$$

Taking the limit in which the infrared regulator μ is set to zero, one rewrites the BDIs in terms of a positive arbitrary constant λ which plays the role of the renormalization group scale

$$I_{\log}(\mu^2) = I_{\log}(\lambda^2) + b \ln\left(\frac{\lambda^2}{\mu^2}\right), \quad b = \frac{i}{(4\pi)^2}. \quad (3)$$

The $I_{\log}(\lambda^2)$ will be subtracted via renormalization, whereas the IR divergent part $\ln(\mu^2)$ must ultimately cancel due to the KLN theorem.

3. NLO corrections to $H \rightarrow gg$ in the large top mass limit

The decay $H \rightarrow gg$ is mainly due to the top quark loop, so we take the limit in which its mass is infinite. Thus, we add the following term to the massless QCD Lagrangian [5, 6]:

$$L_{\text{eff}} = \frac{1}{4} A H G_{\mu\nu}^a G^{a,\mu\nu}, \quad (4)$$

where H is the Higgs boson field, $G_{\mu\nu}^a$ is the field strength tensor of the SU(3) gluon field. The effective coupling $A = \frac{\alpha_s}{3\pi v} (1 + \frac{11}{4} \frac{\alpha_s}{\pi})$ can be obtained by performing the matching of the full theory to its effective version [7–9]. The strong coupling constant is denoted by $\alpha_s = \frac{g_s^2}{4\pi}$ and v is the electroweak vacuum expectation value, $v^2 = (G_F \sqrt{2})^{-1}$ with G_F the Fermi constant. The Feynman rules can be straightforwardly obtained [6].

3.1. UV renormalization

We adopt multiplicative renormalization, rewriting the effective Lagrangian as

$$(L_{\text{eff}})_{\text{ren}} = \frac{1}{4} Z_{\alpha_s} Z_A A H G_{\mu\nu} G^{\mu\nu}, \quad (5)$$

where Z_A and Z_{α_s} are the renormalization constants for the gluon-field and coupling constant respectively. By adopting the Feynman gauge, the counterterm V_{count} to be added to our process is

$$\frac{V_{\text{count}}}{V_0} = \frac{\alpha_s}{b\pi} \left[C_A \left(\frac{5}{12} I_{\log}(\mu^2) - \frac{11}{12} I_{\log}(\lambda^2) \right) - \frac{T_F N_F}{3} (I_{\log}(\lambda^2) - I_{\log}(\mu^2)) \right], \quad (6)$$

where V_0 corresponds to the tree-level amplitude for $H \rightarrow gg$.

3.2. Virtual decay rate

The virtual diagrams contributing to the one-loop order correction are shown in Fig. 1. Momentum-energy conservation $p_1 + p_2 + q = 0$ and the on-shell conditions $p_1^2 = p_2^2 = 0$ are applied throughout the calculations. We

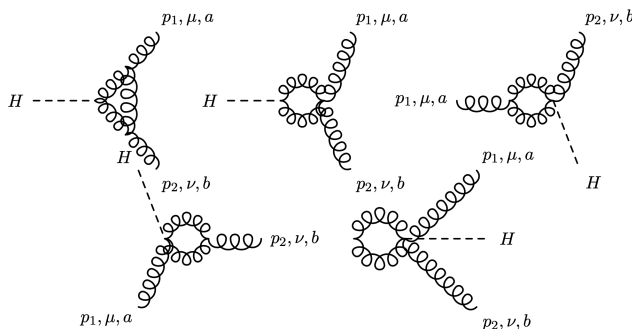


Fig. 1. Virtual diagrams of the decay rate $H \rightarrow gg(g)$. From left to right they are V_1, V_2, V_3, V_4 , and V_5 . The dashed line represents the Higgs field, the curly lines the gluon field. The external momenta are p_1 and p_2 for the gluons, q for the Higgs.

display only the result for the amplitude V_1 as an illustration of the method, see [10] for further details. Defining $\mu_0 = \mu^2/m_H^2$, we obtain

$$\begin{aligned}
V_1 = & Ag^2 C_A \delta^{ab} \left[\left(-I_{\text{quad}}(\mu^2) \left(\frac{13}{2} g^{\mu\nu} \right) \right. \right. \\
& - I_{\text{log}}(\mu^2) \left(-\frac{43}{6} p_1 \cdot p_2 g^{\mu\nu} + \frac{1}{4} p_1^\mu p_1^\nu - \frac{1}{6} p_1^\mu p_2^\nu + \frac{29}{6} p_1^\nu p_2^\mu + \frac{1}{4} p_2^\mu p_2^\nu \right) \\
& + \frac{1}{12} \ln(-\mu_0) \left(-2 p_1^\nu p_2^\mu - \frac{13}{2} p_1 \cdot p_2 g^{\mu\nu} \right) \\
& \left. + \ln(-\mu_0)^2 (-p_1^\nu p_2^\mu + p_1 \cdot p_2 g^{\mu\nu}) - \frac{5}{18} (p_1^\nu p_2^\mu + 4 p_1 \cdot p_2 g^{\mu\nu}) \right]. \quad (7)
\end{aligned}$$

We retain terms up to $\mathcal{O}(\alpha_s^2)$, add all the regularized amplitudes V_i with the counterterm obtained in Eq. (6), and make use of the scale relation Eq. (3), which leads to an UV finite result as expected

$$V_{\text{ren}} = \frac{\alpha_s}{\pi} \left[\left(\frac{11}{12} C_A - \frac{1}{3} T_F N_F \right) \ln \left(\frac{\lambda^2}{\mu^2} \right) \right] V_0. \quad (8)$$

Finally, the virtual decay rate is obtained from the sum of the tree-level amplitude with the one-loop radiative correction

$$\frac{\Gamma_v}{\Gamma_0} = \left[1 + \frac{\alpha_s}{\pi} \left(\frac{11}{2} - \left(\frac{11 C_A}{6} - \frac{N_F}{3} \right) \ln(\mu_0) - \frac{C_A}{2} (\ln(\mu_0)^2 - \pi^2) \right) \right], \quad (9)$$

where we choose the renormalization scale at the Higgs mass ($\lambda^2 = m_H^2$).

3.3. Real decay rate

The diagrams are shown in Fig. 2 (omitting external leg permutation graphs). We use the spinor helicity formalism and refer to [10] for the explicit evaluation. We obtain for the unpolarized total absolute squared amplitude $|\overline{M}|^2 = |\overline{M}_g|^2 + |\overline{M}_q|^2$, where

$$|\overline{M}_g|^2 = A^2 \pi \alpha_s 8 C_A^2 C_F \frac{1}{s_{12} s_{13} s_{23}} (s_{12}^4 + s_{13}^4 + s_{23}^4 + m_H^8) \quad (10)$$

stands for the gluon emission contributions due to the R_1, R_2 diagrams, and

$$|\overline{M}_q|^2 = A^2 \alpha_s 4 \pi C_F C_A \left(\frac{(s_{13}^2 + s_{12}^2)}{s_{23}} + \frac{4 \mu^2 (s_{13} + s_{12})^2}{s_{23}^2} \right) \quad (11)$$

for the gluon and light quark pair emission diagram R_3 . Here, $s_{ij} = (p_i + p_j)^2 = 2 p_i \cdot p_j$ in the massless limit. The last term proportional to μ^2 must

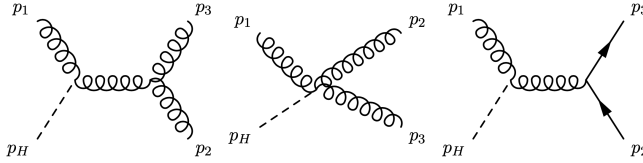


Fig. 2. Real diagrams contributing up to $\alpha_s\sqrt{\alpha_s}$ order to the decay $H \rightarrow ggg$ and $H \rightarrow gq\bar{q}$. From left to right they are R_1 , R_2 and R_3 .

be retained until the integration over the phase space is effected, before taking the limit of vanishing quark masses [10]. The phase-space integral is performed attributing the mass μ to the external particles (gluons and light quarks). The integrals are evaluated using results collected in [1, 11]. The real emission decay rate $\Gamma_{\text{r}}(H \rightarrow gg(g), gq\bar{q})$ is then

$$\frac{\Gamma_{\text{r}}}{\Gamma_0} = \frac{\alpha_s}{\pi} \left[C_A \left(\frac{73}{12} + \frac{11}{6} \ln(\mu_0) + \frac{\ln^2(\mu_0) - \pi^2}{2} \right) + N_F \left(\frac{-\ln(\mu_0)}{3} - \frac{7}{6} \right) \right], \quad (12)$$

where Γ_0 denotes the tree-level decay rate. The final total decay rate $\Gamma_{\text{T}}(H \rightarrow gg(g), gq\bar{q})$ is obtained summing Eqs. (9) and (12). In terms of the renormalization scale λ^2 , which can be left as a free parameter until the very end, $\log(\frac{\lambda^2}{\mu^2}) = \log(\frac{\lambda^2}{m_H^2}) - \log(\mu_0)$, we get in conformity with [9]

$$\frac{\Gamma_{\text{T}}}{\Gamma_0} = \left[1 + \frac{\alpha_s}{\pi} \left(\frac{95}{4} - \frac{7}{6} N_F + \frac{11C_A - 2N_F}{6} \ln \left(\frac{\lambda^2}{m_H^2} \right) \right) \right]. \quad (13)$$

4. Comparison with dimensional schemes

When using DRED, the one-loop contribution due to light quarks can only be consistently obtained when additional operators are taken into account. As we have shown in the previous section, in the case of IReg, the inclusion of ϵ -scalars (or additional operators) is not necessary. Following [12, 13], the virtual contribution to the following decay rates to $\mathcal{O}(\epsilon)$ is [10]:

$$\Gamma_v^{\text{CDR}} = \Gamma_0 \left\{ 1 + \frac{\alpha_s}{\pi} \left[\frac{11}{2} + C_A \left(-\frac{1}{\epsilon^2} - \frac{11}{6\epsilon} + \frac{\pi^2}{12} \right) + \frac{N_F}{3\epsilon} \right] \right\}, \quad (14)$$

$$\Gamma_v^{\text{FDH}} = \Gamma_0 \left\{ 1 + \frac{\alpha_s}{\pi} \left[\frac{11}{2} + C_A \left(-\frac{1}{\epsilon^2} - \frac{11}{6\epsilon} + \frac{\pi^2}{12} + \frac{1}{6} \right) + \frac{N_F}{3\epsilon} \right] \right\}, \quad (15)$$

$$\Gamma_v^{\text{DR}^{\overline{\text{MS}}}} = \Gamma_0 \left\{ 1 + \frac{\alpha_s}{\pi} \left[\frac{11}{2} + C_A \left(-\frac{1}{\epsilon^2} - \frac{11}{6\epsilon} + \frac{\pi^2}{12} \right) + \frac{N_F}{3\epsilon} + \frac{N_F}{6} \right] \right\}. \quad (16)$$

Comparing to Eq. (9), the correspondence $\epsilon^{-1} \rightarrow \log \mu_0$, $\epsilon^{-2} \rightarrow \log^2 \mu_0/2$ applies as first noticed in [1]. The result in CDR does not have any finite term (apart from factors of π^2 that will be cancelled against the real contribution). The same holds true for IReg. For FDH and DRED, on the other hand, there is the appearance of finite terms proportional to C_A and N_F .

Regarding the real contributions, the part proportional to N_F can be readily obtained [10]. For CDR and FDH, only the diagram on the right of Fig. 2 contributes. In DRED, additional operators contribute due to vector boson splitting. The respective decay rates up to $\mathcal{O}(\epsilon)$ are

$$\Gamma_{q,r}^{\text{CDR/FDH}} = \Gamma_0 \frac{\alpha_s}{\pi} \left[-\frac{1}{3\epsilon} - \frac{7}{6} \right] N_F, \quad \Gamma_{q,r}^{\text{DRED}} = \Gamma_0 \frac{\alpha_s}{\pi} \left[-\frac{1}{3\epsilon} - \frac{4}{3} \right] N_F. \quad (17)$$

The result of IReg, Eq. (11), is similar to CDR/FDH in the sense that there is an extra term. In the latter, it comes from extending the physical dimension to d , while in IReg, it is encoded in the fictitious mass that we have added for the massless particles.

5. Conclusion

The decay rate $\Gamma_{\text{T}}(H \rightarrow gg(g), gq\bar{q})$ at α_s^3 order in the strong coupling has been computed in the framework of the fully quadri-dimensional regularization scheme IReg and compared to the dimensional schemes CDR, FDH, and DRED. We achieved not only a full separation of BDI from the UV finite integrals but singled out the IR content as well. By comparing with different dimensional schemes, one concludes that IReg does not require the use of evanescent fields at the one-loop level.

Work supported by FCT projects CERN /FIS-PAR /0040 /2019, CERN /FIS-COM /0035 /2019 and UID /FIS /04564 /2020 — CFisUC, and by CNPq projects 166523/2020-8 and 302790 /2020-9.

REFERENCES

- [1] C. Gnendiger *et al.*, *Eur. Phys. J. C* **77**, 471 (2017).
- [2] T. Kinoshita, *J. Math Phys.* **3**, 650 (1962); T.D. Lee, M. Nauenberg, *Phys. Rev.* **133**, B1549 (1964).
- [3] A. Cherchiglia, M. Sampaio, M. Nemes, *Int. J. Mod. Phys. A* **26**, 2591 (2011).
- [4] A. Bruque, A. Cherchiglia, M. Pérez-Victoria, *J. High Energy Phys.* **2018**, 109 (2018).
- [5] A. Djouadi, M. Spira, P. Zerwas, *Phys. Lett. B* **264**, 1 (1991).

- [6] R.P. Kauffman, S.V. Desai, D. Risal, *Phys. Rev. D* **55**, 4005 (1997).
- [7] T. Inami, T. Kubota, Y. Okada., *Z. Phys. C* **18**, 69 (1983).
- [8] S. Dawson, *Nucl. Phys. B* **359**, 283 (1991).
- [9] M. Spira, A. Djouadi, D. Graudenz, R. Zerwas, *Nucl. Phys. B* **453**, 17 (1995).
- [10] A. Pereira, A. Cherchiglia, M. Sampaio, B. Hiller, *Eur. Phys. J. C* **83**, 73 (2023).
- [11] R. Pittau, *Eur. Phys. J. C* **74**, 2686 (2014).
- [12] C. Gnendiger, A. Signer, D. Stockinger, *Phys. Lett. B* **733**, 296 (2014).
- [13] A. Broggio *et al.*, *Eur. Phys. J. C* **75**, 418 (2015).